

Effective Real Time Attention Bayesian Statistical Methods for Identifying Medical Information Protection

Gyeong-Hyu Seok¹, Bu-Yeon Park², Seol-Kyung Song³, Moon-Sung Jung⁴, Jung-Tae Kim⁵ and Suk-Il Kim⁶

1Dept. of Hospital Medical Information, Cheungam University

2Dept. of Health Service Administration, Seonam University

3Dept. of Dental Hygiene, Seonam University

4Dept. of Real Estate, Seonam University

5Dept. of Real Estate Management, Busan KyungSang College

6Dept. of Child-Care and welfare, DongKang College

dol27@naver.com

Abstract

In this paper, we propose a GRNN(: Generalized Regression Neural Network) algorithms for new eyes and face recognition identification system to solve the points that need corrective action in accordance with the existing problems of facial movements gaze upon it difficult to identify the user and . Using a Kalman filter structural information elements of a face feature to determine the authenticity of the face was estimated future location using the location information of the current head and the treatment time is relatively fast horizontal and vertical elements of the face using a histogram analysis the detected. And the light obtained by configuring the infrared illuminator pupil effects in real-time detection of the pupil, the pupil tracking was - to extract the text print vector. The abstract is to be in fully-justified italicized text as it is here, below the author information.

Keywords: *Bayesian, Neural Networks, Kalman*

1. Introduction

Existing systems use the identification of the line of sight of the face of the movement and eye movement in order to identify the eye. When using only the motion of the face, there is determined the position of the eye based on the location of the face has the drawback cannot detect the subtle changes in gaze. The largest common gaze estimation method based on the research to date is that the pupil based on the relative position between the pupil and the cornea article lint [1-3]. Another problem with eyes and gaze identification systems is that the corrective action necessary with respect to each user. In order to overcome this limitation, the model of the eye [4] proposes a new gaze tracking technology, and two low viscosity, only correction but simplifies the gaze calibration procedure to that required, smooth operation when relatively movement is less by was, it proposes a precise geometric eye model for each user. Also, using the two cameras and the geometric characteristics of the eye and image [5] it is possible to eliminate completely the radial calibration procedure. In this paper, the pupils were tracked in consecutive frames by the Kalman filter algorithm, an object tracking algorithm after the detection of the pupil. 1 to verify that you have correctly identified the primary areas adjacent to the identification result has only enhanced the real-time recognition and identification gaze to re-identify [12-13].

2. Features Using Bayesian Statistical Methods Network

2.1. Bayesian Statistical Methods Network Theory

Bayesian statistical methods networks to learn from one set of data, each node representing each feature of the set of data and each of (arc) has features and represent the dependencies between the probability of the target node based on the Bayesian network in this study typically predictable and [5-7]. Jimyeo the Bayesian statistical methods given network structure consisting of the connection line between each node and the node of the conditional probability, the probability of each node, there is the learning from data can be expressed as a formula the Bayesian statistical methods network as in equation (1.1).

$$p(x) = \prod_{i=1}^n p(x_i | \pi_i) \quad (1.1)$$

Variables A, B, C, D, E, F, and the respective parameters are to have a high value of yes and no, conditional probability Each column of Table 1-1 shows the possible values assigned to the two variables A and B each line represents the probability to have a condition that the variable D yes or no.

Table 1. Conditional Probability Table

	A(y), B(y)	A(y), ~B(n)	~A(n), B(y)	~A(n), ~B(n)
D(y)	0.4	0.1	0.8	0.2
~D(y)	0.6	0.9	0.2	0.8

Bayesian statistical methods use a Bayesian network theory, such as the calculation formula (1.2) probability conditions.

$$P(h|D) = \frac{P(D|h)P(h)}{P(D)} \quad (1.2)$$

When given as the training data set D, P | and (h D) is the posterior probability of h, in order to obtain this P | a (D h), P (h), P (D) should be sought first. Additionally, the maximum posterior probability is the same as equation (1.3).

$$h_{MAP} \equiv \arg \max_{h \in H} P(D|h)P(h) \quad (1.3)$$

Assume that in the absence of both the probability of the maximum likelihood and prior probability of hypotheses and then omitted Ph) value is expressed as equation (1.4).

$$h_{ML} \equiv \arg \max_{h \in H} P(D|h) \quad (1.4)$$

2.2. Face, Eyes with Eye Identification

Because of gradation between the pupil and the iris the difference is very small, it is difficult to have a low accuracy accurate extraction disadvantages [8-9]. Therefore, the movement of the pupil is hard to overcome this disadvantage by extraction tracking using special light such as infrared. Research to obtain the amount of three-dimensional movement of the face is used a method for estimating a three-dimensional rotation amount, and the amount of movement of the face from the motion of the face feature point projected on the two-dimensional camera image as shown in Figure 1 [9-11].

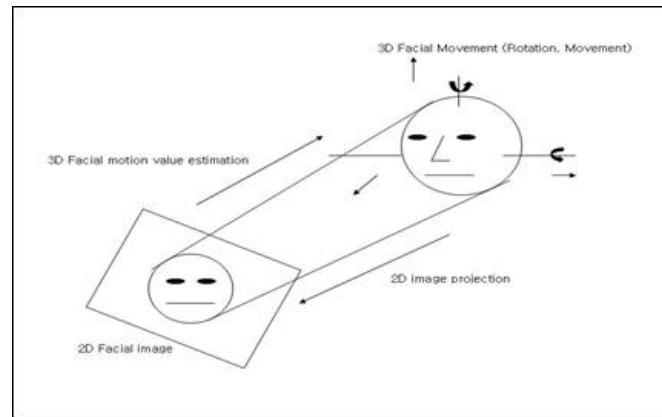


Figure 1. Three-dimensional Movement of the Face Amount of the Estimated

2.3. Face Tracking Feature

Sirovich and Kirby [10] introduced the method applied by the KL transformation for the beardless face image expressing the face. Hallinan [11-12] was used as the template matching to detect the eye image in Figure. In this paper, the detection head area, it is determined whether or not the proper conditions to extract a face candidate region if it is determined. By using the characteristic elements of both eyes, both nostrils and mouth ends of the face, rapid structural information and relatively treatment time horizontal and vertical histogram analysis in order to determine whether or not the face authenticity were detected by the elements of the face. If there is snow two point positions of both eyes appeared a peak position of the histogram in the horizontal and vertical axes are met. For glasses user when extracting eye position, so Eye black pixels may be missing much by the reflection of the spectacle lens, using the binarization upon p-tile method of the eye region a black pixel loss problem by maintaining a constant blackening cow number it was resolved. The nostrils are also extracted in the same way as pupils. In addition, after setting the range for the present position of the mouth by using the structural information of the face is obtained a vertical and horizontal histograms for this zone. Due to the nature of the input vertical histogram is then available in only a portion. The sudden changes in the threshold area is more than the amount of the input end position. Hair region has a characteristic that changes in brightness between neighboring pixels ingredient than the face region and can be expressed as a variance, such as formula (2.1). If the value is more than specified threshold indicates a hair region.

$$V(x, y) = \frac{1}{9} \sum_{i=-1}^1 \sum_{j=-1}^1 |Y(x, y) - Y(x+i, y+j)| \quad (2.1)$$

Image showing the hair region is a hair area 255, and the other is represented by zero. It is possible to obtain a substantial facial area image that is not affected by the hair and the hair image obtained by conventional methods face the logical relationship of the equation (2-2).

$$f_{RF}(x, y) = f_F(x, y) \cap \overline{f_H(x, y)} \quad (2.2)$$

2.4. Artificial Neural Networks for Face Recognition Operation

This research studies the facial recognition algorithm to map GRNN learning. GRNN (: Generalized Regression Neural Network) may leave the base [13] in the observation probability density function of the data to be first used by Specht. Consists of the GRNN is composed of four layers. Type layer (input layer) serves to distribute the input pattern to the neurons in each hidden layer (Hidden Layer) is connected both to the second layer.

The most widely used of the neural network BP (: Back Propagation) because it is connected to the neurons (Neuron) for the axonal synchronization (Axon). The input signal input to the neurons becomes combined after multiplied by the weight associated with each input signal value, the sum is represented as an output value put in a non-linear activation function. In this case BP should use the sigmoid (Sigmoid) function such as equation (3.1).

$$f(x) = \frac{1}{(1 + e^{-x})} \quad (3.1)$$

The calculated output value is used as input data for the next layer or the final output value according to the position of the neurons. Artificial neural networks are thereby varying the connection weights from the square of the error between the measured value and calculated value that is actually required in the artificial neural network sikineunde learning using learning data. The theoretical predictions for what may be the network propagation direction is very difficult, if you obtain a large number of weights, depending on the number of neurons in the hidden layer and the initial weight is difficult to obtain proper results. Subtracting the square of the input layer elements from the training data has shown that each hidden layer neuron or an absolute value. Input function of the j-th hidden layer is equal to the equation (3.2).

$$I_i = \sum_{j=1}^n |W_{ji} - X_{ji}| \quad \text{or} \quad I_i = \sum_{j=1}^n (W_{ji} - X_{ji})^2 \quad (3.2)$$

w_{ji} is the weight between the input signal and w_{ij} is beonjae i type layer and the j-th hidden layer neurons, and n represents the number of neurons in the input layer. This calculated input value is given over to the non-linear activation function having the form of an exponential function such as equation (3.3).

$$f(I_i) = \exp\left(\frac{-I_i}{2\sigma^2}\right) \quad (3.3)$$

Hidden layer the output value of the function calculated on the active layer is passed to the summation, the combined layer by calculating the results by executing the integration of equation (3.4) and sends to the output layer.

$$Y(X) = \frac{\sum_{i=1}^n Y f(I_i)}{\sum_{i=1}^n f(I_i)} \quad (3.4)$$

Y 'corresponds to the result of the learning data by the output value having the respective hidden layer neurons. Summarizing the above procedure as follows. GRNN is input to the network in each of the learning phase are used to calculate the response to the new input value. And it places the Gaussian kernel function on each learning stage. The result value calculated by the input value is calculated by placing a weight in the resulting average value of the learning phase, the weights are related to the learning phase with the calculated value. Great advantage compared to the back propagation GRNN is having the learning data is relatively less that required is the point. If wave reversal learning data of about 1% in order to obtain similar accuracy have to [13], and the training data is large, it can be used to populate a similar data.

2.5. Probabilistic Graphical Models

When modeling a biological system and an entity associated with the gene expression level system is treated as a random variable of the probabilistic model (4). Random variables include the expression level of the gene, such as shown in the model, such as the hidden characteristics and gene array experiments. The probability distribution model is coupled to all the random variables that exist and probabilistic graph model representing the structure of the associated output exhibits a joint probability distribution of a multi-variate only a small number of variables in a graph in accordance with the output of the threshold. The graph is because it is associated with a variable that represents the general

limitations This graph is a tool for specifying the production form of distribution and to deduce the characteristic indicated by the artifacts, and (5) expression in scattered graph efficient inference and learning processes.

Figures 2 and probability using a hierarchical configuration properties of the network graph to the probability recognition in molecular biology, such as graphs and network discovery proves graph to stochastic signal path that demonstrate the biological signaling pathways and the number of incoming edges of each node as because it has an outgoing edge appears about five times the proven navigation in the actual network.

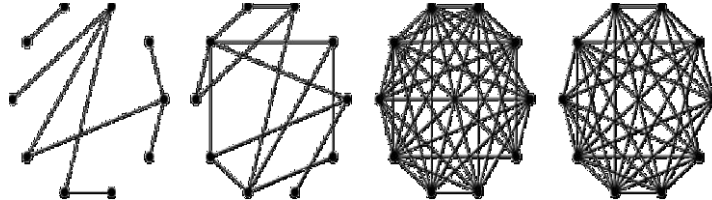


Figure 2. Network Search Graph

Probabilistic graph in Figure 2 is capable of complex objects is so extended in a multi-tiered network as evidenced by the probability search object representation because it can deal with all of the stochastic surface and the surface of the structural object. The lower layer, it is possible to demonstrate the expression of the underlying information, and the upper layer using the learned model searching goes up to the upper layer by the probabilistic inference information from the network which can be obtained by a combination of lower layers of the object.

The so achieved by the characteristics of the stochastic search proved graphs and information is stochastic method such as expression navigation recognition so made the result output from the stochastic graph to model a biological system with a set of derived [1.6] edge network node probabilistic network graph is defined as follows.

Definitions 1 (network graph) An network graph over $A_V \cup A_E$ is a 4-tuple $G = (V(G), E(G), \phi, \varepsilon)$ such that

- ✓ $V(G)$ is a finite, nonempty set of vertices;
- ✓ $E(G) \subset V(G) \times V(G)$ is a set of ordered pairs of distinct elements in $V(G)$, called edges;
- ✓ A_V is a finite, nonempty set of vertex labels (primitive descriptions);
- ✓ A_E is a set of edge labels (relation descriptions);
- ✓ $\phi: V(G) \rightarrow A_V$ is a function, called a vertex interpreter;
- ✓ $\varepsilon: E(G) \rightarrow A_E$ is a function, called an edge interpreter.

The network graph using the above definition consists of the vertices and edges in terms probability parameter a probabilistic graph condition variable in a certain way that is used to represent the characteristics of the recognition target network itself, and connect the stochastic component values at each vertex and edge thereby to generate a probabilistic network graph. $G = \langle N, E \rangle$ is the probability La probabilistic graph output by the probability function $U = (v, \delta)$, R in the graph, the output from the probability G , R is so expressed as the product of the output probability edge G following formula (4.1).

$$P_R(G, U) = \prod_{\alpha \in W} P_r(\nu = v'(\alpha_i)) \prod_{B_i \in B} P_r(b = \delta'(B_i) | \nu = v'(\alpha_k)) \quad (4.1)$$

However, $\alpha \in N, \beta \in E$ and δ', μ' is the inverse of each μ and δ and $U = (u, \delta)$ is a probability function to convert $\mu: N \rightarrow R_N$ and $\delta: E \rightarrow R_E$ Equation (1) it can be obtained at home, and is independent of any direction except the vertices and edges in the probabilistic graph. Output probability in equation (4.1) is obtained by multiplying the probabilities of the probability of the vertices and edges.

Numerical biology chain graph consists of a set of stochastic nodes and edges can be applied to stochastic modeling proved in that multi-day probability is possible. Definition of the chain graph is similar to the definition of a biologically probability graph, but it can be inferred that some features have been matched to have the network-to-network-forming cells probabilistic edge. The biological probability distributions will recognize that the probability distribution model, indicating that many of the features that are matched. As a result, the edges of the biological probability distribution chain graph being used to model the length and direction of a node is the probability distribution to model a stochastic type of connection between networks.

Since the biological probability distribution chain graph to produce a large number because statistically processing information output probability is the probability network $P(X|U)$ liver cells as the product of all of the nodes and the edge probability is the same as equation (4.2).

$$P(X|U) = \sum_{\gamma} P(X, \gamma|U) \quad (4.2)$$

Since the above equation U and X is probabilistic model and γ are probabilistic functions chain to all the nodes and edges from the probability as equation (4.3).

$$P(X, \gamma|U) = \prod_{\alpha \in X} P(\alpha = \Phi(\alpha)) \prod_{\nu \in X} P(B = k(\nu) | \forall \alpha \in A_{\beta} \supseteq \alpha \in A_{\nu}, A = \Phi(\alpha)) \quad (4.3)$$

Φ in equation (4.3) is a biological probability edge mapping function, \mathcal{K} is a set of probability edges connected at node mapping function, aa is an edge, ν is the node, a is the probability edge, β probability nodes, A_{β} probability node β , A_{ν} is a set of probabilistic network is connected to the edge node ν . Liver cells in order to find the network input to the probability $P(X|U)$ to this approach is too complicated, since in reality model. Although this is an inference value it has not yet been proven that it is described as significantly different from the original value deemed to be not much different from the reasoning in $\max_{\gamma} P(X|U), P(X|U)$.

New inference model presented and, because it is probabilistic model representing the biological signal path to the upper layer in the probabilistic hierarchical representation based on the reasoning model the signal path in order to express the elements of a stochastic layer based on the gene shared layer distribution model represents a probability for the cell position relationship between a network.

Figure 3 is a probabilistic cross-path models because two basic probabilities to 32, using the coupling between the distribution because it induced a network node of the

cross-path probabilistically cross paths with a probability distribution combined with gene combination into a circle probability distribution by configuring the parameters of the edge node and there exists a probability distribution for the biological cross-path direction of the edge in the stochastic model. Node of the two edge portions is connected, there is a probability distribution network chain between cells in the coupling between the two edges.

Matching of the combined probability distribution model is a chain of points of contact and kkeok stochastic graph of each cell and the cells in a matching process to be done first in the recognition between cells, cell recognition. Extracting an edge representing a biological cross-path connections among the chains to the vertex so that a probability function application to obtain a probabilistic graph can have two probabilities in the probabilistic model graph cell portion can be derived as follows.

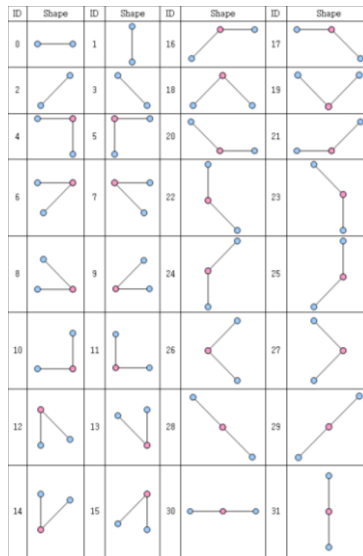


Figure 3. The Probability Distribution Model which is Combined with the Gene

In Figure 3, since this distribution to learn and as close as possible to the model of the observed basal an inference model to study parameter estimation with the model selection is a parameter of the conditional probabilities for the model structure. In the model selection, so that best reflect the dependency of the area so are selected from a variety of model structures maximized so that the discrete optimization problem well matched to the data [6] was, to predict the random variable values to calculate a matching distribution [7] was selected.

3. Kalman Filter Algorithm Applied

3.1. Kalman Filter and Pupil Tracking Using the Moving Average Algorithm

Using an eye tracking apparatus using a bright pupil based on a Kalman filter to determine the location of the pupil in the initial frame and track bright pupil by the Kalman filter. The movement of the pupil in each frame is characterized by a rate of change in the pupil. (c_t, r_t) if the position of the pupil center of the pixel at the time t and referred to at the time t (u_t, v_t) speed change of direction to the c and r , can be expressed at a time point t to the state vector $x_t = (c_t, r_t, u_t, v_t)^T$. And the system can be modeled as follows:

$$X_{t+1} = \Phi X_t + W_t \quad (5.1)$$

wt represents the imperfection of the system. When considered from the point in time t for the pupil position in $Z_t = (\hat{c}_t, \hat{r}_t)$, the measurement model can be obtained by the Kalman filter.

$$z_t = Hx_t + v_t \quad (5.2)$$

In formula 4.2 vt is an indeterminate measurement. Obtaining the estimated position to be a bright pupil effect is estimated by using a threshold value in adjacent pixels. Obtaining an initial value of the state vector and covariance matrix Σ_{t+1} , x_{t+1} is an updated system model and the measurement model for the prediction.

If the snow during a cold pupil tracking Kalman filter or disappear into a bright pupil by an obstruction, so the disadvantage becomes impossible to track by the Kalman filter, using the moving average algorithm increased the accuracy of eye tracking.

Average tracking algorithm is repeated moving average by measuring the similarity of two intensity distributions with a bar according to the similarity factor Tara chiya to find the most similar model and candidate regions. Bata's perked estimated coefficients for the target density q in the Y branch and calculate the density of the target candidate.

$$\tilde{p}(y) = p[\tilde{p}(y), \tilde{q}] - \sum_{\alpha=1}^m \sqrt{p_{\alpha} \tilde{q}_{\alpha}} \quad (5.3)$$

The distance for the two distributions are:

$$d(y) = \sqrt{1 - p[\tilde{p}(y), \tilde{q}]} \quad (5.4)$$

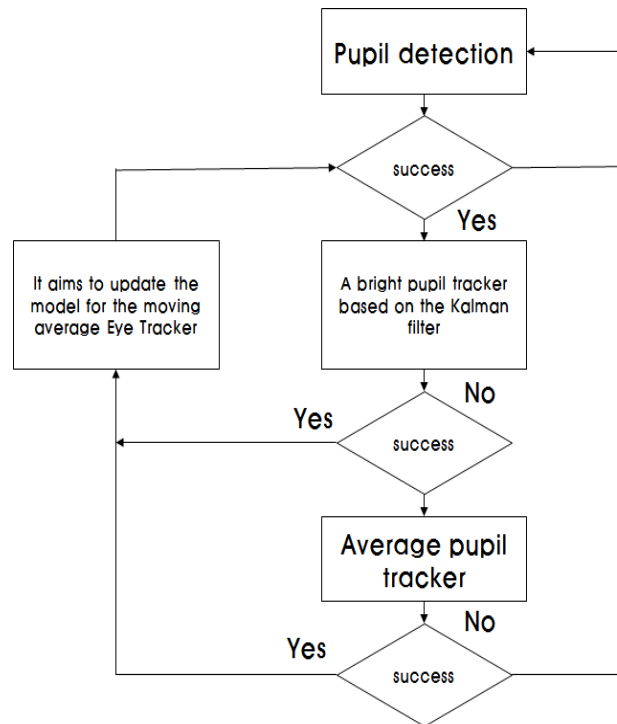


Figure 4. Pupil Tracking Algorithm

Characteristics of the intensity distribution in a region other than the snow and are built quite characteristic by two images even and odd fields. Obtaining a probability distribution of two different characteristics corresponding to a dark pupil image and a bright pupil may lead to a two-dimensional combined histogram.

Table 2. Compare Pupil Tracking

300 Picture frame		Kalman Filter Tracker		The proposed synthetic tracker	
		Recognized frames	Recognition	Recognized frames	Recognition
Left Eye	2260 frame (Open eye)	2012	89%	2255	99%
	330 frame (Close eye)	0	0%	317	95%
	410 frame (Hidden eye)	0	0%	384	94%
Right eye	2125 frame (Open eye)	1945	92%	2117	99%
	330 frame (Close eye)	0	0%	307	93%
	545 frame (Hidden eye)	0	0%	499	92%
Recognition		3957	66%	5879	98%

3.2. Face Identification Preprocessing

This paper was irradiated with infrared rays at an intensity of 32mW to produce an active infrared illuminator configured the IR LED wavelength of 880nm as the two ring-shaped on the basis of the method of Hutchinson 40nm in wavelength to obtain a pupil image. For users wearing glasses can be misrecognized due to the reflection of light in the 0.5 ~ 1m was assumed to be the case if you were not wearing the glasses to the camera and your distance you sit naturally in front of a computer. When the infrared LED of the inner ring are turned, as cross-examine the light source is reflected infrared rays from the pupil detected was a bright pupil image generation, when infrared LED on the outer ring are turned on is not the reflected infrared pupil detected dark the pupil was produced. Using the even field image and an odd field, background, and external light such create an image, but the pupil of the even field brighter than the odd field showed, background and the difference image by removing the odd-numbered field image on the even-numbered field image to eliminate the interference of external light made. Interference effects in the majority of the background and the external light has been removed in the difference image.

3.3. Extraction Parameter

When using only the primary parameter to identify the eye itgie tend not performed well in the case of identifying the line of sight with the movement In this paper, we want to extract the parameters for the face direction against the face moves. Pupil characteristics of the face direction is as follows. □ face as it rotates from the front side to narrow the distance between the pupil. □ average contrast ratio of greater than one or two pupils than one face while rotating from side to side or up and down. □ is smaller shape than the two pupils are elliptical, while the face is rotated horizontally or vertically. □ size of the pupil becomes smaller, while the face is rotated horizontally or vertically. This use as a basis for estimating the face direction from the pupil, the left and right pupil size, the right and left pupillary distance and the parameter so that by using the right and left pupil contrast, such as right and left pupil shape by analyzing the face direction such features

may have a consistency It was normalized by dividing the measured value of the variables in the front face. The problem with the method proposed in this paper, is that it cannot be made the identification of a pupil when the pupil is covered by the eyelid. In order to address this problem, the facing direction by the average value be calculated for a point in time, including before and after the face direction measurement for the frame. Also requires empirical constraints such as the assumption that the movement of the head workable nature, as the face direction measured, before and after the point.

3.4. Gaze Correction

In order to identify the eye with a pupil and print articles obtained from pretreatment pupil it was ever perform a function that maps the article lint on the monitor vector-vector and configure the print paper, the pupil. Find the pupil and post print parameters according to which the only function if the parameters of the pupil and articles Lint given enough attention by the GRNN was to generalize the campus.

Input vector to be used for GRNN is as follows.

$$q = \Delta x \Delta y \tau \theta q_x q_z \quad (4.5)$$

Article lint-pupil size vector is also associated with the distance of the built-in infrared illuminator camera and the subject. By moving the face and calculating a pupil face movement and pupil movement update as a parameter to meet it, it is possible to reduce the impact of the head movement. Further parameters were able to effectively remove the re-calculation for other users can be generalized because it is independent of the line of sight with respect to the mapping function of the pupil size.

4. Results and Discussion

4.1. Facial Motion Classification Analysis

The detected facial feature was used to analyze the facial expression and to determine the movement of each element. Total five awake patient intended for sitting on in the state each room or carelessness with the same set-up as yawning, and estimates the face eye region according to the amount of change of the face and eyelids like jamdeum. Experimental Experiments environment by using the infrared camera system, a total of approximately 1 minute record the face image 5 times with 320 * 240 resolution, 20 frames per second. At this time, the set prior probabilities for all classifications in the bottom-up steps careless yawn, jamdeum in the same operation. Eye detection area for the experiment, head direction estimating head motion estimation, assuming an operation in a combination of face tracking, such as a, b, c, d, e, f, and for carelessness, yawning, jamdeum all steps in each operation a pre-probability measures. Ia, Yw, Fa denote carelessness, yawn, sleep deumeul.

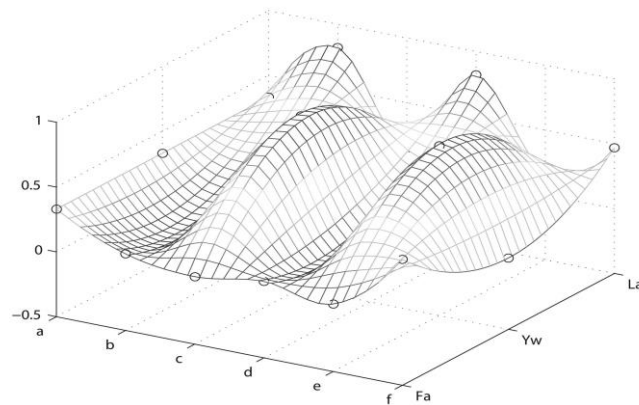


Figure 5. Face Motion Classification

In Figure 5 a was measured I_a , Y_w , F_a values are equal to a value smaller than 0.33 to 0.5. This means the state without a change in the operating face when the wakefulness or arousal. b exhibited a high prior probability of the state inadvertently. c This measurement was 0.83 Y_w is highly applicable to yawn and d and e are each measured by careless yawn and classification results. That is, a, b, c, d, e is easy to gaze detected in the face region according to various operations of the subject. But f 0.47 was measured in the same manner as the prior probability and a careless jamdeum.

To help identify the gaze position on a monitor by configuring the abduction ever fixture in real-time detection of the pupil obtained a bright pupil effect was traced.

4.2. Re-identification Recognition Results for Adjacent Areas

Experimental results on user not involved in the study were identified as a whole indicate the rate of approximately 84%. 3,6 and 4,5 times the area adjacent area is represented in many cases the misrecognized adjacent areas. It is understood that the recognition rate than participating in the study are significantly degraded and cannot see that you have identified adjacent to correctly identify the actual gaze area. 23% of 18% of eyes looking at the area 1 is misrecognized eyes looking at the three areas appear as two areas have been identified as areas 4.

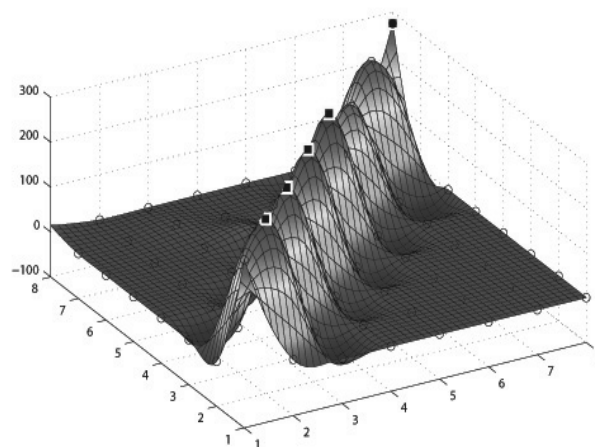


Figure 6. Line Identification Result Using a Material Identifier

As a result, the misrecognized mainly occurs in areas adjacent gaze. Please check the neighboring area for each eye region and perform learning by using only learning data of the adjacent region, so as to re-identify an adjacent area with only verifies the identification result. If it is not the case of the material is improved identification accuracy than 9% was achieved by 93% accuracy. In particular, in error rate was 8% at 18% of the area between the adjacent 1 and 2, the error rate in the area between the eyes 3 and 4 was reduced from the previous 24% to 5%. Also improved error misrecognized by the eye area or other exhibited the same performance. By the generalized corrective action through the eyes GRNN requires no calibration for the individual, even if the movement of the face will be a great advantage because it operates reliably.

5. Conclusion

In this paper, by using the Kalman filter using the location information of the current head it was estimated future location is determined whether or not the proper state when the judgment after the hair area detection candidate regions are extracted face. Using both eyes, both nostrils of characteristic elements of the face, by using the ends of the structural information and the mouth relatively fast horizontal processing time, a vertical histogram analysis in order to determine whether or not the authenticity of the face was detected in the face elements. To track the iris and the pupil area are accurate extraction because of the advantage that can be implemented easily without the special light required because tracking the movement of the pupil by the image processing method under normal lighting, but smaller gray level is also very different between the pupil and the iris there is difficult and the accuracy low. Therefore, to identify the location on the eye monitor to configure the IR illuminator obtained a bright pupil effect real-time detect the pupil, the pupil tracking was-extracted with the article lint vector.

Experimental results quantizes the monitor coordinates in $4 * 2$, to suggest a gaze identification system operating correctly if the face moves, without calibration, a user not involved in the study of the 2400 frames when there is movement of the face It was to identify the right eye with respect to the 2075 frames scored accuracy of about 84%, as a result of the analysis that is not recognized correctly result was found with respect to the adjacent areas that are misrecognized. Therefore, by the re-identification for reducing the misrecognized character in the identification results were ever validate the eye region. When it re-identifies the line of sight of the adjacent regions in the study in error rate was 8% at 18% of between 1 and 2, between 3 and 4 the error rate was decreased from 24% to 5% is increased by about 9% degree of accuracy than the conventional 84% exhibited a 93% accuracy. Proposed Line identifier was identified to improve the performance of the real-time line of sight, or if the calibration according to the user with no natural facial movements. In the future, studies should overcome the limitations of the user's requirements Glasses Come spatial resolution and high attention to further refine your eye area.

Acknowledgements

This paper is a revised and expanded version of a paper entitled [Effective Real-time Identification using Bayesian Statistical Methods Gaze Network] presented at [Proceedings International Conferences, August 19-20, 2016, Harbin, China, NGCIT 2016].

References

- [1] J. Lee, K. Jeong, G. Park, and K. Sohn, "A Quantitative Reliability Analysis of FPGA-based Controller for applying to Nuclear Instrumentation and Control System", J. of the Korea Institute of Electronic Communication Sciences, vol. 9, no. 10, (2014), pp. 1117-1123.
- [2] K. Sung and T. Poggio, "Example-based learning for view-based human face detection", IEEE Transactions on Pattern Analysis and Machine Intelligence, vol. 20, no. 1, (2008), pp. 39-51.
- [3] T. Yamaguchi, M. Tominage, K. Mrakami and H. Koshimizu, "Regeneration of facial image eye-contacting with partner on TV Conference environment", IEEE International Conference on Systems, Man, and Cybernetics, vol. 2, (2006), pp. 1169-1174.
- [4] M. Faruqe and M. Hasan, "Face Recognition Using PCA and SVM", Anti-counterfeiting, Security, and Identification in Communication, 2009. ASID 2009. 3rd Int. Conf. on, Hong Kong, (2009), pp. 97-101.
- [5] J. Yang and J. Yang, "Why can LDA be performed in PCA transformed space?," Pattern Recognition vol. 36, no. 2, (2003), pp. 563-566.
- [6] V. Napnik, "The Nature of Statistical Learning Theory", New York: Springer-verlag, (1995).
- [7] P. Liao, J. Liu, M. Wang, J. Ma, and W. Zhang, "Ensemble local fractional LDA for Face Recognition," Computer Science and Automation Engineering(CSAE), 2012 IEEE Int. Conf. on, Zhangjiajie, China vol. 3, (2012), pp. 586-590.
- [8] C. Liu and H. Wechsler, "Independent component analysis of Gabor feature for face recognition", IEEE Trans. Neural Networks, vol. 14, no. 4, (2003), pp. 919-928.
- [9] S. E. El-Khamy, O. Abdel-Alim, and M. M. Saii, "Neural Network Face Recognition Using Statistical Feature Extraction", Radio Science Conf., 2000. 17th NRSC '2000. Seventeenth National, Minufiya, (2000), pp. C31/1-C31/8.
- [10] E. Osuna, R. Freund, and F. Girosi, "Training Support Vector Machines: An application of face detection", Proceeding IEEE. Computer Society Conference on. Computer Vision and Pattern Recognition (CVPR), San Juan, Puerto Rico., (1997), pp. 130-136.
- [11] M. Yang, "Kernel Eigenfaces vs. Kernel Fisherfaces: Face Recognition Using kernel Methods, Automatrix Face and Gesture Recognition", 2002, Proceeding Fourth IEEE Int. Conf., Washington D.C., U.S.A., (2002), pp. 0215.
- [12] H. Kim, "Vocal Separation in Music Using SVM and Selective Frequency Subtraction", J. of the Korea Institute of Electronic Communication Sciences, vol. 10, no. 1, (2015), pp. 1-6.
- [13] J. Jo, "A Car License Plate Recognition Using Colors Information, Morphological Characteristic and Neural Network", J. of the Korea Institute of Electronic Communication Sciences, vol. 5, no. 3, (2010), pp. 304-308.
- [14] H. Park, "A User Adaptation Method for Hand Shape Recognition Using Wrist-Mounted Camera", J. of the Korea Institute of Electronic Communication Sciences, vol. 8, no. (2012), pp. 204-212.
- [15] G. Seok, "Effective Real-time Identification using Bayesian Statistical Methods Gaze Network", Proceedings International Conferences, 2016, Harbin, China, vol. 138, (2016), pp. 38-43.

Authors



Gyeong-Hyu Seok, received his MS, and PhD degrees in Computer Science in 1997, and 2005, respectively, from the Chosun University, Korea. He joined Cheongam College, where he is currently as professor in the department of Hospital Medical Information. His research interests include optical security, Data Communication Systems, Hospital Network, Neural Network and biomedical engineering.



Bu-Yeon Park, received his MS, and Ph.D degrees in Public health in 2005, and 2012, respectively, from the Chosun University Korea. He joined Seonam University, Where he is currently as associate professor in the department of hospital administration. his research interests include EMR, PACS and OCS



Seol-Kyung Song, received her MS, degrees in Health Science in 2004, respectively, from the Wonkwang University, Korea. She joined Seonam University, where she is currently as professor in the department of Dental Hygiene.



Moon-Sung Jung, received his LL.B., and LL.M., LL.D. degrees in Law in 1989, 1992, and 2003, respectively, from the Honam, Jeonju University, Korea. He joined Seonam University, where he is currently as associate professor in the department of Security Service and Private investigation. His research interest Intellectual Property Rights, Regulations of Food Hygienics, Health & Medical Administration.



Jung-Tae Kim, received his MS, and PhD degrees in Real Estate, Private Law of Property in 2001, and 2008, respectively, from the Dong-Eui University, Busan National University. He joined Busan Kyungsang College, where he is currently as associate professor in the department of Real Estate Management. His research interests include Private Law of Property, Real Estate Policy, and Atomic Energy Relation Law.



Suk-II Kim, received she is PhD degrees in Journalism from Chngang University, Korea in 2015, respectively. She joined Dongkang College, where she is currently as associate professor in the department of Child and welfare. She is research interests include Child development, health and safety management, program development and evaluation of infant child.